Pramana – J. Phys. (2022) 96:59
https://doi.org/10.1007/s12043-021-02273-z

Noise-formed triple-well potential and stochastic resonance of charge carriers

BERHANU ARAGIE[1], MULUGETA BEKELE[2] and GIUSEPPE PELLICANE[3,4,5],*

[1]Department of Physics, CCNS, Wolkite University, P.O. Box 007, Wolkite, Ethiopia
[2]Department of Physics, Addis Ababa University, P.O. Box 1176, Addis Ababa, Ethiopia
[3]Dipartimento di Scienze Biomediche, Odontoiatriche e delle Immagini Morfologiche e Funzionali, Universita degli Studi di Messina, 98125 Messina, Italy
[4]CNR-IPCF, Viale F. Stagno d'Alcontres, 37-98158 Messina, Italy
[5]School of Chemistry and Physics, University of Kwazulu-Natal and National Institute of Theoretical Physics (NIThEP), Pietermaritzburg 3209, South Africa
*Corresponding author. E-mail: gpellicane@unime.it

MS received 7 April 2021; accepted 6 September 2021

Abstract. We study the thermal dynamics of charge carriers jumping across potential traps in a one-dimensional semiconductor layer. The potential traps are denser at the middle layer and decay exponentially when moving away from it. Such a distribution drives the diffusion of the charge carriers toward the centre. Then, the application of a non-uniform temperature, hotter around the centre, gives a chance for some of the charge carriers to spread out. Exposing the system to an external bistable potential, more intense at the two ends of the semiconductor layer, forces the outward-moving charge carriers to condense around two localised positions. As a result, charge carriers are dense in the central region and in two symmetrically positioned regions away from the centre. Using numerical simulation, in the framework of three-state approximation, we investigate the mobility of charge carriers as a function of different controlling parameters. In the presence of two time-varying signals, we calculate explicitly the transition rates from the middle layer towards the edges of the semiconductor layer and vice versa. We also study the stochastic resonance by monitoring the asymmetric mean position of the charge carrier distribution, that is triggered by the synchronisation of signals with the noise-driven transition.

Keywords. Charge carriers diffusion; triple wall potential; stochastic resonance.

PACS Nos 05.60.–k; 05.40.–a

1. Introduction

Diffusion is a mechanism that plays a pivotal role in the fabrication of semiconductor devices such as transistors and diodes. A major breakthrough was the development of ion implantation where small amounts of a specific type of dopant are added at particular locations, with tight control of dopant depth. As a result, there has been a dramatic enhancement of their properties, including conduction that depends on the type of dopant, concentration of the dopant and temperature [1,2].

Conduction by hopping is the most important mechanism occurring at low temperature, where charge carriers jump from a potential trap to another one. A potential trap in an n-type semiconductor is formed by localised, empty donors. Since, at sufficiently low temperature, most of the electrons are recaptured by the donors, electrons hop directly from occupied donors to empty ones in the impurity band. Ion implantation technique can be used to create an imbalance in the concentration of donors, i.e., a small number of occupied donors and a large number of empty donors.

The mobility of charge carriers in semiconductors can be manipulated by varying the concentration of impurities, the strength and shape of the temperature profile and the external potential energy function, along the semiconductor layer. Conduction can also be altered by applying a time-varying signal, that may determine the onset of stochastic resonance (SR), where the diffusivity of charge carriers gets amplified.

In general, SR provides a way to amplify weak input signals with the help of noise. SR has been observed experimentally in different systems including bistable electronic circuits [3–6], ring lasers [7], Schmitt triggers [8] and so on. It has been widely studied numerically during the last three decades in the framework of linear response theory. Recently, stochastic resonance in multiwell systems received considerable attention by the scientific community because triple-well systems are found in many areas of chemical kinetics and condensed matter physics [9,10]. A statistical model for thermal diffusion of charge carriers by hopping in a non-homogeneous medium has been originally introduced by van Kampen [11]. Within that model, we have studied the dynamics of impurities hopping through potential traps under thermal noise in one-dimensional [12–16] and two-dimensional semiconductor layers [17]. We found that the competition between a non-homogeneous temperature gradient and a monostable external potential can generate a steady-state Boltzmann probability distribution of the impurities, where the effective potential energy function resembles a double-well potential. The latter triggered a redistribution of charge carriers around two points symmetrically positioned with respect to the centre of the semiconductor layer. Very recently, we showed that the composition of a Gaussian and inverted Gaussian temperature distribution, in the presence of a homogeneous traps distribution, can also determine the accumulation of charge carriers around two regions. Then, within a two-state model approximation in the presence of slowly time-varying signals of small amplitude, we were able to study the SR of the model [12–17].

Since the control over the diffusion of impurities to a desired region is of paramount importance in semiconductor physics, in this paper we present a new approach to facilitate transportation and distribution of charge carriers under non-uniform thermal noise. We neglect the interaction between the dopants at low impurity density and assume the existence of a non-homogeneous trap distribution, which is peaked in the proximity of the central region of the semiconductor layer. The spatial distribution of impurities can be controlled experimentally by using ion current and implantation time. The application of a temperature gradient, hotter around the centre, forces some of the charge carriers to diffuse towards the colder regions. The last perturbation we apply is a bistable potential, more intense at the two ends of the semiconductor layer, which triggers localisation of charge carriers in two symmetric regions with respect to the centre. This potential energy function can be realised through split or square gates, which have the advantage of preserving the crystal structure, as diffusion can take place at low temperature. For instance, Narayan and Willander [18,19] provided evidence of how a harmonic potential can be generated via metallic gates at the top of the semiconductor layer, which are kept at a certain voltage. What makes our work even more relevant is the recent progress in the field, that made possible the generation of an external double-well potential in semiconductor devices with a suitable geometry and fine-tuning of the voltage of the electrostatic gates [20,21].

Then, we show that the probability distribution of charge carriers becomes maximum at the middle point of the layer and at two symmetric points away from it, i.e. there are three regions more densely populated with charge carriers. We study the distribution of charge carriers using different controlling parameters. When the system is perturbed with two slowly varying signals of small amplitude, stochastic resonance takes place. Using numerical simulation within the three-state approximation, we investigate the spatial changes of the mean position of the charge carriers distribution.

The remaining part of the paper is constructed as follows. In §2, we explain the model. In §3, we study in detail the diffusion and distribution of charge carriers. We also study the asymmetric transition rate, towards and from the centre of the semiconductor layer, as a function of the input signal frequency. In §4, we show the results for the stochastic resonance of charge carriers. Summary and conclusions are reported in §5.

2. The model

Let us consider a one-dimensional semiconductor layer in which potential traps are non-homogeneously distributed. Charge carriers hop from one potential trap to the neighbouring one, each having potential depth Φ, in units of $k_\mathrm{B}T_0$, due to thermal noise. The traps are denser around the centre and decay exponentially as we move away from it. Let us use as unit of length the generic length L. The medium contains a trap distribution with density $\Omega\sigma(x)$. Their mutual distances are of the order of Ω^{-1}, which set the microscopic length-scale. $\sigma(x)$ is defined as

$$\sigma(x) = \exp\left(-\frac{x^2}{2b_1^2}\right), \tag{1}$$

where x is the distance from the centre of the semiconductor layer and the parameter b_1 is the standard deviation of the distribution. Both quantities are reported in units of L.

Then, a reduced (dimensionless) one-dimensional external bistable potential energy $V_\mathrm{ext}(x)$ given by

$$V^*_\mathrm{ext}(x) = \frac{V_\mathrm{ext}(x)}{k_\mathrm{B}T_0} = \frac{V_0}{k_\mathrm{B}T_0}x^2(x^2-a^2), \tag{2}$$

is applied along the semiconductor layer, as shown in figure 1 (right), where T_0 is an arbitrary temperature, k_B is the Boltzmann constant and a is in units of L. The energy barrier is higher at the centre and even higher at the two ends of the semiconductor.

Finally, a reduced (dimensionless) non-uniform background temperature

$$T^*(x) = \frac{k_B T(x)}{V_0} = \frac{k_B T_0}{V_0(x^2+b^2)}, \tag{3}$$

is applied, which is peaked at the centre as shown in figure 1 (left) and where the parameter b is in units of L. The temperature hot spot at the centre decreases as moving away along both sides of the semiconductor layer, which pushes some charge carriers to diffuse far from the central region.

The dynamics of the system is governed by the following equation:

$$\frac{\partial P(x,t)}{\partial t} = \frac{c}{\Omega^2}\frac{\partial}{\partial x}\left\{\frac{V'_{\text{ext}}(x)}{k_B T\sigma^2}\exp\left(-\frac{\Phi}{k_B T}\right)P(x,t) + \frac{1}{\sigma}\frac{\partial}{\partial x}\left[\frac{1}{\sigma}\exp\left(-\frac{\Phi}{k_B T}\right)P(x,t)\right]\right\}. \tag{4}$$

According to van Kampen [11], the steady-state probability distribution $P_{ss}(x)$ becomes

$$P_{ss}(x) = C\sigma(x)\exp\left[\frac{\Phi}{k_B T(x)}\right]\exp\left[-\int_0^x \frac{V'_{\text{ext}}(y)}{kT(y)}\mathrm{d}y\right], \tag{5}$$

where C is the normalisation factor and the presence of $\sigma(x)$ implies that the stationary density is proportional to the number of available traps; the third factor is the probability of occupation of each trap and the last factor takes into account the effect of the external field. The rearrangement of the above equation gives the steady-state probability distribution $P_{ss}(x)$ as

$$P_{ss}(x) = C_0 \mathrm{e}^{-\frac{V_{\text{eff}}(x)}{k_B T_0}}, \tag{6}$$

where the effective potential $V_{\text{eff}}(x)$ is given by

$$V_{\text{eff}}(x) = \frac{2}{3}V_0 x^6 - \left(\frac{1}{2}a^2 - b^2\right)V_0 x^4 + (\kappa - V_0(ab)^2 - \Phi)x^2 \tag{7}$$

and $\kappa = k_B T_0/2b_1^2$. This effective potential is a triple well potential formed because of the combined effect of the external bistable potential and non-homogeneous nature of the trap and temperature distributions across the layer. The effective potential reported in eq. (7) is a triple-well potential where the following conditions are met:

$$\frac{1}{2}a^2 > b^2, \tag{8}$$

$$\kappa > V_0((ab)^2 + \Phi) \tag{9}$$

and

$$\left(\frac{1}{2}a^2 - b^2\right)^2 > \frac{2}{V_0}(\kappa - V_0(ab)^2 - \Phi). \tag{10}$$

In that case, the system becomes equivalent to a distribution of charge carriers under the effect of an effective triple-well potential with a uniform distribution of traps and temperature. The saddle points of this effective triple-well potential are located at two symmetrically-positioned points from the centre:

$$x_{\pm} = \pm\left\{\frac{1}{2}\left[\left(\frac{1}{2}a^2 - b^2\right) - \sqrt{\left(\frac{1}{2}a^2 - b^2\right)^2 - \frac{2}{V_0}(\kappa - V_0(ab)^2 - \Phi)}\right]\right\}^{1/2}. \tag{11}$$

The three local minima are positioned at $x = 0$ and at the two symmetrically-positioned points:

$$x_{m\pm} = \pm\left\{\frac{1}{2}\left[\left(\frac{1}{2}a^2 - b^2\right) + \sqrt{\left(\frac{1}{2}a^2 - b^2\right)^2 - \frac{2}{V_0}(\kappa - V_0(ab)^2 - \Phi)}\right]\right\}^{1/2}. \tag{12}$$

The three wells of the effective triple-well potential are at the same depth when

$$\Delta V_{\text{eff}}(L,R) = \Delta V_{\text{eff}}(M), \tag{13}$$

where $\Delta V_{\text{eff}}(L,R)$ ($\Delta V_{\text{eff}}(M)$) is the potential barrier height from the left (right) to the centre and, accordingly

$$V_{\text{eff}}(x = x_{m\pm}) = V_{\text{eff}}(x = 0) = 0. \tag{14}$$

Let us see in the next section how the potential well depth and width change under the effect of different controlling parameters.

3. Charge carrier distribution and transition rates

Consider a small concentration of non-interacting charge carriers in an n-type semiconductor layer at low temperature. The non-homogeneous distribution of potential traps is formed because of the presence of empty donors at sufficiently low temperature. The concentration of the dopant should be small enough to avoid correlation between the dopants, so that localisation of electronic states in the impurity atoms takes place, which is the microscopic origin of the trap potential. The semiconductor layer is doped with a small concentration of acceptors via ion implantation, making possible a large number of empty donors at low temperature. Thus, conduction takes place by hopping of charge carriers between donor states in the impurity band and thermally activated tunnelling between impurity sites becomes the

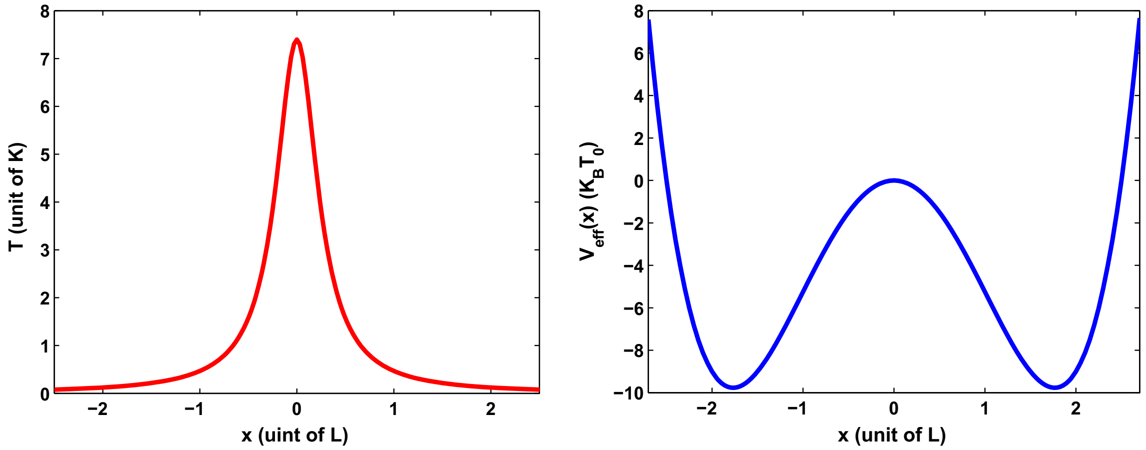

Figure 1. (*Left panel*) Reduced non-uniform temperature $T^*(x)$ as a function of x for parameters $(k_B T_0/V_0) = 0.5$ and $b = 0.26$. (*Right panel*) One-dimensional bistable reduced potential energy $V^*_{\text{ext}}(x)$ for $a = 2.5$ and $(V_0/k_B T_0) = 1$.

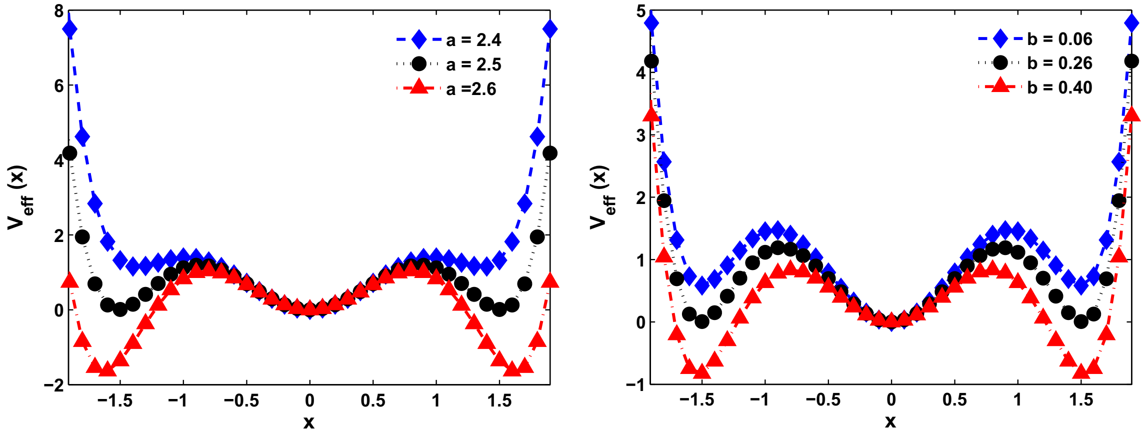

Figure 2. (*Left panel*) Effective potentials (in units of $k_B T_0$) for $a = 2.4$ (diamonds), $a = 2.5$ (circles), $a = 2.6$ (triangles). Calculations are reported for $\Phi = 1.9$, $\kappa/V_0 = 5.8$ and $(V_0/k_B T_0) = 1$. (*Right panel*) Effective potentials for $b = 0.06$ (diamonds), $b = 0.26$ (circles), $b = 0.4$ (triangles). Calculations are reported for $\Phi = 1.9$, $a = 2.5$ and $(V_0/k_B T_0) = 1$.

dominant conduction mechanism. The spatial distribution of impurities can also be controlled by manipulating ion current and implantation time, so as to achieve a denser potential trap distribution near the centre, which forces charge carriers near the central region.

At this stage, the combined effect of a non-homogeneous temperature gradient and the external bistable potential pushes electrons away from the centre and make them populate two new, symmetric positions from the semiconductor middle layer. Thus, charge carriers get distributed around three regions, like a system under the action of an effective triple-well potential, as long as conditions reported in eqs (8)–(10) are obeyed, but in the presence of a homogeneous medium and uniform temperature. Let us discuss how this system behaves and what the distribution of charge carriers looks like when several controlling parameters are varied inside a meaningful, physical range.

When a increases, the well depth and width of the two symmetrically-positioned wells from the middle layer of the external, bistable potential reported in eq. (2) become, respectively deeper and larger, while the potential value at the top of the energy barrier in the middle layer is always equal to 0. As shown in figure 2 (left), the well depth and width of the two symmetrically-positioned wells of the effective potential reported in eq. (7) follow the same trend of the underlying, external bistable potential, as a increases. The depth of the central well remains almost unaltered, which allows the charge carriers to more easily escape from the middle well to the two lateral wells. Similarly, the depth and width of two lateral wells of the effective potential

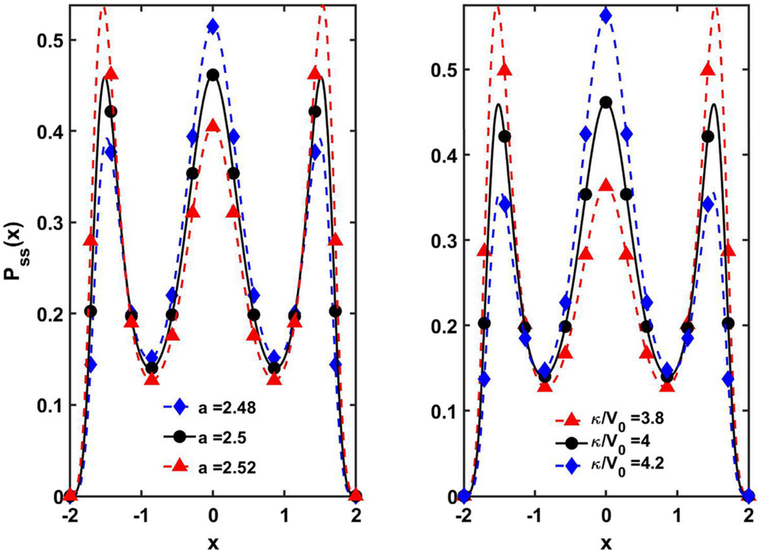

Figure 3. (*Left panel*) Steady-state probability distribution as a function of position for parameters $a = 2.52$ (diamonds), $a = 2.50$ (circles), $a = 2.48$ (triangles). Other parameters are: $\kappa = 4$, $\Phi = 0.07$, $b = 0.26$ and $(V_0/k_B T_0) = 1.0$. (*Right panel*) Steady-state probability distribution as a function of position for parameters $\kappa/V_0 = 3.8$ (diamonds), $\kappa/V_0 = 4.0$ (circles), $\kappa/V_0 = 4.2$ (crosses). Other parameters are: $a = 2.5$, $\Phi = 0.07$, $b = 0.26$ and $(V_0/k_B T_0) = 1.0$.

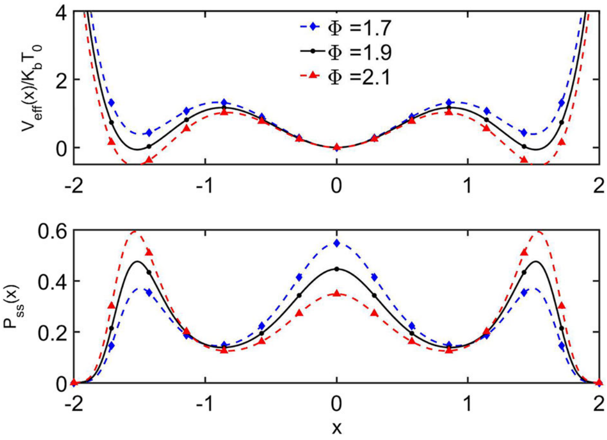

Figure 4. (*Top panel*) Effective potentials for different values of Φ. Other parameters are: $a = 2.5$, $b = 0.26$, $\kappa/V_0 = 5.8$ and $(V_0/k_B T_0) = 1$. (*Bottom panel*) Distribution probability for the same parameters.

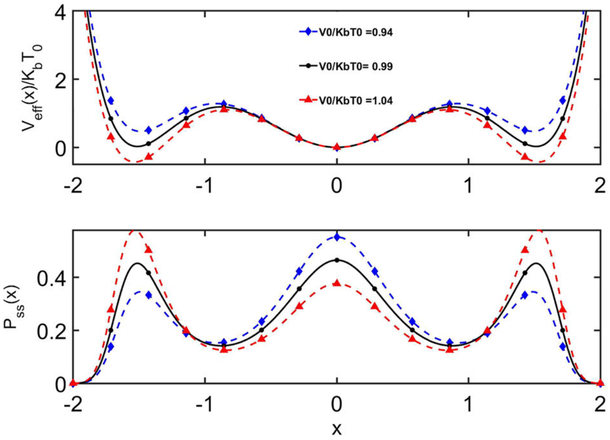

Figure 5. (*Top panel*) Effective potentials for different values of $(V_0/k_B T_0)$. Other parameters are: $a = 2.5$, $b = 0.26$, $\kappa/V_0 = 5.8$ and $\Phi = 1.91$. (*Bottom panel*) Distribution probability for the same parameters.

increase when b increases (see figure 2 (right)), which corresponds to the temperature distribution becoming shallower, according to eq. (3). In general, the same effect (data not shown here) can be obtained by tempering with the parameter κ, by increasing parameter b_1, i.e. by making the impurity distribution broader (see eq. (1)), or decreasing the hot-spot temperature T_0, both of which make κ smaller. Then, the combined effect of increasing a and decreasing κ, shrinks the depth of the middle well significantly, nearly changing the triple-well potential to a double-well potential with minima symmetric with respect to the centre of the semiconductor layer. Conversely, decreasing a and increasing κ, makes the triple-well potential nearly degenerate into a single-well potential, with a minimum in the centre of the semiconductor layer.

As it is visible in the two panels of figure 2, while the increase of a or b makes the two symmetric wells broader and deeper, that feature is also accompanied by the increase of the distance between the two minima (which is more evident for the range variation of parameter a, as reported in figure 2 (left)).

In general, all parameters a, b, Φ, κ and V_0 can be used to control the well depth and the distance between the two symmetric wells from the middle well of the triple-well potential. These parameters in turn generate different charge distributions around the three wells. For example, when the total number of charge carriers entering the middle potential minimum becomes the same as the total number of charge carriers leaving it, the steady-state probability of the charge carrier distribution becomes the same around the three wells, as shown in figure 3 (see the black curve on both left and right panels). In the same figure, we show that by increasing the value of a, the probability for a charge carrier to be localised at the two lateral wells becomes higher because they become deeper, and the higher barrier height makes it difficult for the charge carriers to overcome it. As the total number of charge carriers is fixed, the increase of the population around the two lateral wells results in a decrease in the population of charge carriers around the middle well, which is reflected in the steady-state probability (see the blue curve of figure 3 (left)). A decrease of the parameter a from the case of equiprobability of the three wells, make the opposite to happen and the steady-state probability of the middle well becomes higher than the one of the symmetric wells. In figure 3 (right), we show the same mechanism with increase (decrease) of κ from the case of equiprobability of the three wells.

It is interesting to note that changing the trap potential depth Φ to some extent produces a similar effect of changing the parameters a or b (see figure 4). In fact, increase of any of the parameters Φ, a or b, will shift the effective potential to a bistable potential. However, the triple-well potential will not lose its nature with further decrease in Φ and b. We report the ability of the effective potential to be controlled by variations of trap energy Φ, by showing the transition from the absolute minimum of the effective potential in the centre of the semiconductor layer to the two symmetric positions away from it, in figure 4. Finally, we show that even the depth V_0 of the external potential can be used for the same purpose in figure 5.

Let us investigate how the thermally activated barriers alter the transition rate of charge carriers (crossing rate) from the middle well outwards and vice versa, while changing the input signal frequency and controlling the parameters. Here we assume that the non-interacting charge carriers are initially localised around the middle well. By increasing the temperature, the transition rate of charge carriers increases both inwards (towards the middle well) and outwards (towards the symmetric wells). We consider the application of two periodic signals, one additive and the other multiplicative. The additive signal A_1 forces the external potential wells side-wise, whereas the multiplicative signal A_2 causes a symmetric oscillation of the barrier heights.

The two signals are of small amplitude (that allows us to use the approximation of high barrier limit) and very slowly varying ones. $A_1(t)$ and $A_2(t)$ are such that $\Delta V_{0\to x_\pm} \gg A_1, A_2$ and $\Delta V_{x_\pm \to 0} \gg A_1, A_2$, where $\Delta V_{0\to x_\pm}$ and $\Delta V_{x_\pm\to 0}$ are the thermally activated barriers for charge carriers crossing outwards and inwards, respectively. We assume that time is measured in units of τ and the frequency ω in units of τ^{-1}. The Kramer's escape time (the inverse of Kramer's rate) outwards $1/R_{0\to x_\pm}$ and inwards $1/R_{x_\pm\to 0}$ for the unperturbed system is much smaller than the time period of the external input signals: $1/R_{0\to x_\pm} \ll 2\pi/\omega_1$, $1/R_{0\to x_\pm} \ll 2\pi/\omega_2$, $1/R_{x_\pm\to 0} \ll 2\pi/\omega_1$ and $1/R_{x_\pm\to 0} \ll 2\pi/\omega_2$, where ω_i is the frequency of the signal labelled as i. Then, we can write the expressions for the time-dependent crossing rates outwards as follows:

$$W_M^L = R_{x=0\to x=x_{m_-}} \exp\left(-\frac{A_1 x_- \sin(\omega_1 t+\phi_1) - \frac{A_2 x_-^2}{2}\sin(\omega_2 t+\phi_2)}{D}\right) \tag{15}$$

$$W_M^R = R_{x=0\to x=x_{m_+}} \exp\left(\frac{A_1 x_+ \sin(\omega_1 t+\phi_1) + \frac{A_2 x_+^2}{2}\sin(\omega_2 t+\phi_2)}{D}\right), \tag{16}$$

and inwards as

$$W_R^M = R_{x=x_{m_+}\to x=0} \exp\left(-\frac{A_1 (x_{m_+}-x_+) \sin(\omega_1 t+\phi_1) - \frac{A_2 (x_{m_+}^2-x_+^2)}{2}\sin(\omega_2 t+\phi_2)}{D}\right) \tag{17}$$

$$W_L^M = R_{x=x_{m_-}\to x=0} \exp\left(+\frac{A_1 (x_{m_-}-x_-) \sin(\omega_1 t+\phi_1) + \frac{A_2 (x_{m_-}^2-x_-^2)}{2}\sin(\omega_2 t+\phi_2)}{D}\right), \tag{18}$$

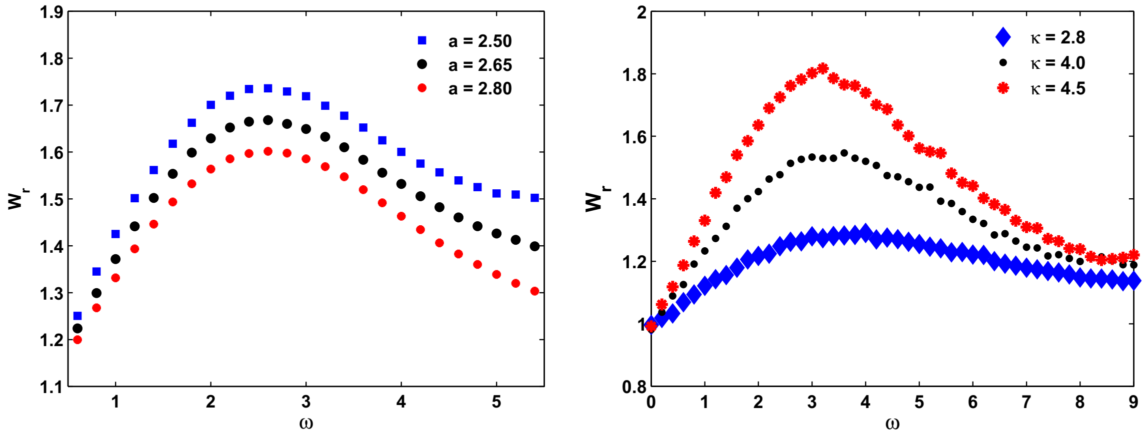

Figure 6. (*Left panel*) Ratio of transition rates right–left vs. frequency for parameters $a = 2.4$ (diamonds), $a = 2.5$ (dots), $a = 2.7$ (stars) (here $\kappa/V_0 = 4$ and $(V_0/k_B T_0) = 1$). (*Right panel*) Ratio of transition rate right–left vs. frequency for parameters $\kappa/V_0 = 2.8$ (diamonds), $\kappa/V_0 = 0.26$ (dots), $\kappa/V_0 = 4.0$ (stars) (here $\Phi = 4.5$ and $(V_0/k_B T_0) = 1$)

where

$$R_{x_{m\pm}\to x=0} = \frac{\sqrt{|\omega_{x=x_{m\pm}}||\omega_{x=x_\pm}|}}{2\pi} \times \exp\frac{-[V(x=x_\pm) - V(x=x_{m\pm})]}{k_B T_0},$$

$$R_{x=0\to x_{m\pm}} = \frac{\sqrt{|\omega_{x=0}||\omega_{x=x_\pm}|}}{2\pi} \times \exp\frac{-[V(x=x_\pm) - V(x=0)]}{k_B T_0}$$

are the Kramer's rate of particle transitions from one well to the other in the absence of a periodic force, $D = k_B T_0$ and the subscripts L, R, M stand for left, right and middle respectively. Thus, in our analysis of thermal diffusion of charge carriers, we consider them undergoing a random walk motion along the effective potential subject to thermal kicks of magnitude equal to D.

We estimate numerically the ratio of transition rates outwards to the right W_M^R and to the left well W_M^L, i.e. $W_r = (\langle W_M^R\rangle/\langle W_M^L\rangle)$ as a function of driving frequency under the condition $\omega_1 = \omega_2 = \omega$ and $\phi_1 = \phi_2 = 0$. We consider three discrete states in which charge carriers are allowed to be positioned. Initially, we add 10000 non-interacting charge carriers at the middle well. We select all the charge carriers in every site at every time instant. We choose randomly the direction to which the charge carrier will be allowed to hop and then we compare the transition probability with a generated random number between 0 and 1. Finally, we count the number of charge carriers found in the left well (n_L) and right well (n_R) and we calculate the average ratio W_r over different instants of time and with different input signal frequencies.

When the input signals synchronise, the barrier height in the right side of the middle well potential becomes minimum due to the force A_2, responsible for the symmetric oscillation of the potential heights and the force A_1, responsible for shifting the potential wells sidewise, being directed to the right well. Moreover, the tilting force A_2 in the left side also causes the barrier height to reach a maximum value which makes it difficult for the charge carriers to diffuse towards the left well. Then, more charge carriers from the middle well immediately move towards the right and W_r becomes greater than one.

We show W_r vs. the frequency of input signals (ω), for different controlling parameters in figure 6. W_r attains a maximum peak at a particular ω. Upon decreasing the parameter a the peak shifts to lower frequencies and becomes higher, as shown in figure 6 (left panel). This is due to the lifting down of the potential minimum on the right side, that makes the barrier height smaller, as well as lifting up of the potential minimum on the left side, that makes the barrier height higher, as the parameter a decreases. This feature makes the crossing of the energy barrier easier for the charge carriers from the middle well to the right and difficult from the middle to the right well. Conversely, as shown in figure 6 (right panel) increasing κ makes the peak of W_r smaller and and also shifts toward higher frequencies.

When b decreases, the value of W_r follows a similar trend to the one shown for a. This happens because after synchronisation of input signals, the barrier height between the middle and the left sided wells lowers down. As a result, charge carriers can hop more easily from the left side to the middle well, while the peak of W_r becomes enhanced and shifts to lower frequencies, as b decreases (data not shown here). A similar behaviour is observed when Φ decreases (data not shown here).

4. Stochastic resonance of charge carriers

co In this section, we consider the stochastic resonance (SR) which occurs when time-varying signals we considered in the previous section, becomes synchronised with the noise-assisted system subjected to a triple well potential. The most important effect of the appropriate matching of the intensity of thermal noise, in the presence of the external signal, is that the system may exhibit the maximum number of charge carriers passing through the barrier height. The rationale behind SR is that the applied signal makes each state less stable than the other, by alternatively raising and lowering the potential wells over the half forcing period. Then, by matching the forcing angular frequency ω with the interwell transition rate induced by thermal noise, SR occurs and a large portion of charge carriers is more likely to be found inside the more stable well. In other words, the charge carrier attains the maximum probability of escaping out of the less stable state.

In our system, synchronisation of forces A_1 (pushing the potential wells along the semiconductor layer) and A_2 (determining a transverse oscillation to the semiconductor layer) with thermal noise brings the energy barrier height down to a minimum and shifts it towards the right direction. This dynamical effect causes the charge carriers to spend most of their time between the middle and the right wells, by generating an asymmetry of the stochastic localisation in the two wells. So, asymmetric mean position measurement of charge carriers is a possible way of studying stochastic resonance. Obviously, the interwell transition rate depends on noise intensity, i.e. thermal noise. So, we shall discuss the mean position $\langle x \rangle$ of the charge carriers as a function of thermal noise, by fixing different controlling parameters.

To perform numerical simulation, we considered a single charge carrier with arbitrary starting position among the three possible states. The trajectories of the charge carrier were allowed to evolve dynamically for a long time. Then, by sampling the transition rate probabilities as in the previous section, we could obtain the probability of site occupation of the charge carrier and calculate the mean position along the semiconductor layer. Our simulation parameters were $\omega = 0.008$, $\mathrm{d}t = 0.009$, $A_1 = 0.08$ and $A_2 = 0.21$.

Figure 7 (left panel) shows the variation of the mean position of the charge carrier with temperature, for different values of a. With increasing temperature, the mean position initially increases and then gradually decreases, after it attains a maximum value. Increasing the value of a results in higher values of the mean position peak. This effect is obviously associated with the deepening of the potential well on the right side, that becomes the most probable location of charge carriers with increasing a. Furthermore, the peak position shifts to the left with increasing a. A similar behaviour is observed when b increases, as shown in figure 7 (right panel).

In figure 8 (left panel), we show the behaviour of $\langle x \rangle$ with varying κ. The peak of $\langle x \rangle$ becomes higher with decreasing κ and the optimal value of T_0 also shifts to the left, as κ decreases. This shows that the mean position to the background noise strength is significant at lower values of κ, i.e. when the trap distribution becomes broader (κ is inversely proportional to b_1). The mean position when Φ is varied, shows a similar trend to what is already observed for the changes of a and b (see figure 8 (right panel)).

Let us now suggest a possible experimental set-up of this numerical work. Using ion implantation, one can generate a Gaussian distribution of potential traps by adding dopant in the region of interest. Of course, to deplete the resulting built-in internal field and to avoid any correlations between the dopant, it is necessary that the doping level is low. During the doping process, it is important to use layers of oxide [22] because the oxide layer also functions as a reflector at the edge of the semiconductor layer. Since conduction by hopping in the impurity band takes place at low temperature, there should exist a small number of occupied donors due to a mechanism of donor–acceptor compensation [23],which facilitates thermally activated tunnelling between impurity sites as the dominant conduction mechanism. Once the semiconductor layer with the desired properties is prepared, the last step is to add a hot-temperature reservoir around the central region and a bistable potential with saddle point at the centre, with the help of electronic split gates. As a result, we should obtain three regions where charge carriers get more densely populated. Then, slowly varying AC signals of small amplitude can be applied to the material. By varying the appropriate controlling parameters, the system may show SR, in which an asymmetric distribution of charge carriers takes place and a fast transportation of impurities occurs without the need of exposing them to a high temperature. Such experimental set-up should be useful to study the nature of mobility of charge carriers in a semiconductor layer, under small thermal stress and should be able to amplify weak signals.

It is important to note that negatively biased metallic gates with respect to side gates on the top of a semiconductor heterostructure device can confine electrons

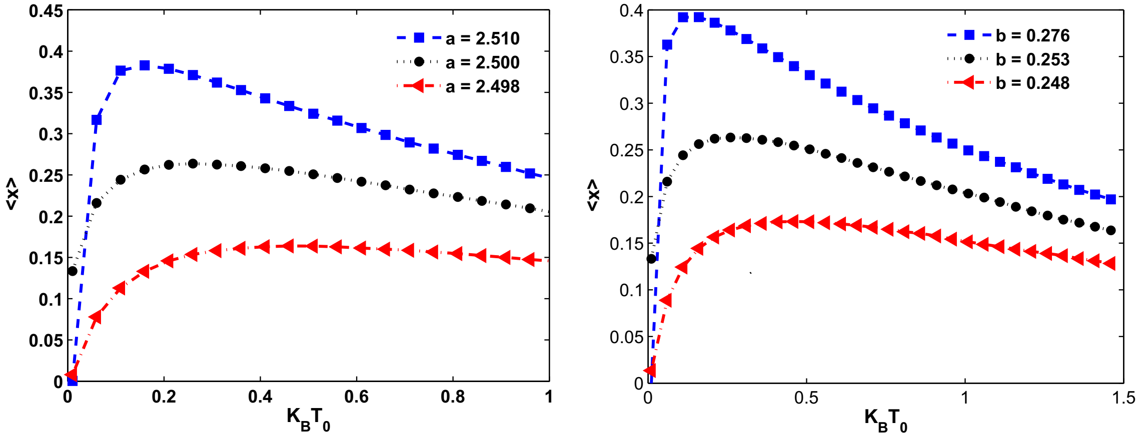

Figure 7. (*Left panel*) Mean position vs. $(k_{\mathrm{B}}T_0/V_0)$ for parameters $a = 2.520$ (squares), $a = 2.500$ (circles), $a = 2.480$ (triangles). Here $b = 0.26$. (*Right panel*) Mean position vs. $(k_{\mathrm{B}}T_0/V_0)$ for parameters $b = 0.29$ (squares), $b = 0.26$ (circles), $b = 0.21$ (triangles). Here $a = 2.5$. Other parameters are fixed as $\kappa = 4$, $\omega = 0.0008$, $\Phi = 0.07$, $A_1 = 0.08$, $A_2 = 0.21$ and $\mathrm{d}t = 0.009$.

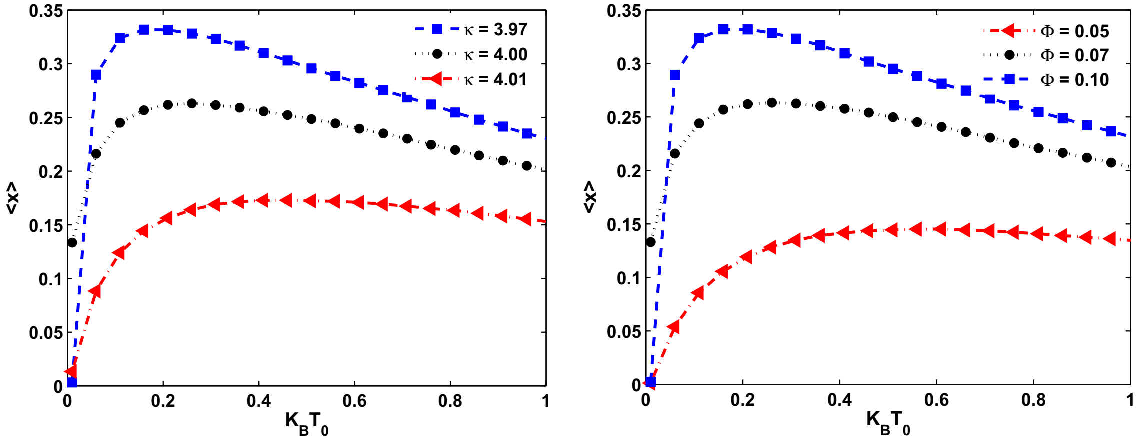

Figure 8. (*Left panel*) Mean position vs. $(k_{\mathrm{B}}T_0/V_0)$ for parameters $a = 2.520$ (squares), $a = 2.500$ (circles), $a = 2.480$ (triangles). Here $b = 0.26$. (*Right panel*) Mean position vs. $(k_{\mathrm{B}}T_0/V_0)$ for parameters $b = 0.29$ (squares), $b = 0.26$ (circles), $b = 0.21$ (triangles). Here $a = 2.5$. Other parameters are fixed as $\kappa = 4$, $\omega = 0.0008$, $\Phi = 0.07$, $A_1 = 0.08$, $A_2 = 0.21$ and $\mathrm{d}t = 0.009$.

in a quasi-one-dimensional quantum wire and in some confinement conditions an external double-well potential as the one we use in our model can be generated [20]. An electrostatic potential with a double well structure created by electrostatic gates was also generated in tunnel-coupled wires made from semiconductor heterostructure [21].

5. Conclusions

In this numerical work, we studied the thermal dynamics of non-interacting charge carriers hopping across potential traps, in a one-dimensional semiconductor layer. The potential traps are non-homogeneously distributed and more dense around the central region. A non-uniform temperature, hotter at the centre and the application of a bistable potential, stronger at the two ends of the semiconductor layer, forced the outward-moving charge carriers to redistribute around two new regions, finally resulting in three regions where charge carriers are more densely populated.

The system can be mapped into a one-dimensional semiconductor under the effect of a homogeneous trap distribution and a uniform temperature, subjected to a triple-well potential. The outer well depths of the effective triple-well potential increases with increasing depth of the bistable potential and trap potential depth and decreasing temperature at the centre, or shrinking of the variance of the trap distribution. This effect is the origin of the depletion of charge carrier distribution in the centre of the semiconductor layer. By studying the transition rates of charge carriers in the high barrier limit, under the effect of two periodic signals, we have shown that the maximum rate becomes higher and more asymmetric with decrease in the variance of the trap distribution, depth of the bistable potential and trap potential depth and with increase in the variance of the trap distribution. We have also shown that the system perturbed by the two periodic signals of small amplitude can exhibit stochastic resonance, by monitoring the mean position of charge carriers as a function of the thermal energy.

The model we studied in this paper is useful to highlight different approaches for improving the diffusion of charge carriers in a semiconductor layer and it also shows potential for being used to detect slowly varying signals of very small amplitude.

Acknowledgements

GP acknowledges the South African Centre for High Performance Computing (CHPC) and Dr A Lopis for assistance and granting access to computational resources under the allocation MATS0887.

References

[1] M B Prince, *Phys. Rev.* **93**, 1204 (1954)
[2] B Abeles, *Phys. Rev.* **131**, 1906 (1963)
[3] M Borromeo and F Marchesoni, *Phys. Rev. E* **81**, 012102 (2010)
[4] S Fauve and F Heslot, *Phys. Lett. A* **97**, 5 (1983)
[5] A R Bulsara, M E Inchiosa and L Gammaitoni, *Phys. Rev. Lett.* **77**, 2162 (1996)
[6] A Nitkin, N G Stocks and A R Bulsara, *Phys. Rev. E* **68**, 036133 (2003)
[7] B McNamara, K Wiesenfeld and R Roy, *Phys. Rev. Lett.* **60**, 2626 (1988)
[8] F Marchesoni, A Apostolico and S Satucci, *Phys. Rev. E* **59**, 3958 (1999)
[9] P K Ghosh, B C Bang and D S Ray, *J. Chem. Phys.* **127**, 044510 (2004)
[10] F Bouthanoute, L El Arroum, Y Boughaleb and M Mazroui, *Moroc. J. Phys.-Condens. Matter* **9**, 17 (2007)
[11] N G van Kampen, *J. Phys. Chem. Solids* **49**, 673(1988)
[12] B Aragie, Yergou B Tateka and M Bekele, *Eur. Phys. J. B* **87**, 101 (2014)
[13] B Aragie, M Asfaw, L Demeyu and M Bekele, *EPJB* **87**, 214 (2014)
[14] B Aragie, *J. Comput. Theor. Trans.* **48(1)**, 36 (2019)
[15] B Aragie, *J. Comput. Theor. Trans.* **49(2)**, 88 (2020)
[16] B Aragie, *Int. J. Mod. Phys. B* **28**, 1550011 (2014)
[17] M Asfaw, B Aragie and M Bekele, *Eur. Phys. J. B* **79**, 371 (2011)
[18] V Narayan and M Willander, *Phys. Rev. B* **65**, 125330 (2002)
[19] V Narayan and M Willander, *Phys. Rev. B* **65**, 075308 (2002)
[20] E T Owen and C H W Barnes, *Phys. Rev. Appl.* **6**, 054007 (2016)
[21] S Kumar, K J Thomas, L W Smith, M Pepper, G L Creeth, I Farrer, D Ritchie, G Jones and J Griffiths, *Phys. Rev. B* **90**, 201304(R) (2014)
[22] D A Neamen, *Semicondutor physics and devices: Basic principles* (McGraw-Hill, New York, 2003)
[23] J Zhang, W Cui, M Juda, D McCammon, R L Kelley, S H Moseley, C K Stahle and A E Szymkowiak, *Phys. Rev. B* **48**, 2312 (1993)